

**Fluid Dynamics and Heat Transfer in a Hartmann Flow**

by

Timothy Richard DePuy

An Engineering Project Submitted to the Graduate

Faculty of Rensselaer Polytechnic Institute

in Partial Fulfillment of the

Requirements for the degree of

MASTER OF ENGINEERING IN MECHANICAL ENGINEERING

Approved:

---

Ernesto Gutierrez, Project Adviser

Rensselaer Polytechnic Institute  
Hartford, Connecticut

December, 2010

# CONTENTS

LIST OF SYMBOLS .....	iii
LIST OF TABLES .....	iv
LIST OF FIGURES .....	v
ABSTRACT .....	vi
1. Introduction.....	1
2. Methodology.....	2
2.1 Governing Equations.....	2
2.2 Solution Method.....	5
2.2.1 Lorentz Force Solution.....	5
2.2.2 Hydrodynamic Flow Solution.....	7
2.2.3 Heat Transfer Solution.....	9
2.3 Expected Results .....	10
3. Results and Discussion .....	12
3.1 Lorentz Force Solution.....	12
3.2 Fluid Flow Solution .....	14
3.3 Heat Transfer Solution .....	15
4. Conclusions.....	19
4.1 Applicability of COMSOL to MHD Flows .....	19
4.2 Heat Transfer in Hartmann Flows.....	20
5. References.....	21
6. Appendix A: Additional Graphs of Solutions .....	22

## LIST OF SYMBOLS

D, Electric Displacement Field ( $C/m^2$ )

$\rho_e$ , Free Charge Density (C/m)

P, Pressure (Pa)

$\mu, \mu_f$ , Viscosity (Pa\*s)

H, Magnetizing Field (A/m)

J,  $J_x, J_z$ , Current Density ( $A/m^2$ )

$\mu_0$ , Magnetic Permeability ( $N/A^2$ )

M, Hartmann Number

V,u,v,w, Velocity (m/s)

B,  $B_0, B_x, B_z$ , Magnetic Fields (T)

E,  $E_x, E_z$ , Electric Field (N/C)

$\sigma$ , Electrical Conductivity of the Fluid (S/m)

$F_b$ , Body Force (N)

$D_h$ , Hydraulic Diameter (m)

Re, Reynolds Number

Pr, Prandtl Number

$q''$ , Heat Flux ( $W/m^2$ )

T, Temperature (K)

$\rho$ , Density ( $kg/m^3$ )

$c_p$ , Heat Capacity ( $J/(kg*K)$ )

k, Thermal Conductivity ( $W/(m*K)$ )

h, Convective Heat Transfer Coefficient ( $W/(m^2*K)$ )

$i$ , Static Enthalpy (J)

$\gamma_j$ , Mass Diffusion Coefficient

$m_j$ , Mass Concentration

$Q$ , Heat Source (J)

## LIST OF TABLES

Table 1. Applicable Fluid Properties of Mercury at 523K .....	5
Table 2. Conditions Used to Evaluate the Lorentz Force Contribution .....	6
Table 3. Conditions Used to Evaluate the Fluid Velocities.....	8
Table 4. Conditions Used to Evaluate the Magnetic and Hydrodynamic Models.....	12
Table 5. Post-processed Heat Transfer Results .....	18
Table 6. Nusselt Numbers for Parallel Plate Flow Versus Entry Length .....	18

## LIST OF FIGURES

Figure 1. Electric and Magnetic Fields Applied to a Pressure Driven Parallel Plate Flow	2
Figure 2. Meshed Domain .....	5
Figure 3. Applied Magnetostatics Boundary Conditions .....	6
Figure 4. Iterative Solution Method.....	7
Figure 5. Applied Fluid Dynamics Boundary Conditions .....	7
Figure 6. Transition to Turbulence in Hartmann Flows [9].....	9
Figure 7. Applied Boundary Conditions for the Heat Transfer Analysis .....	9
Figure 8. Calculated and Exact Lorentz Force Solutions .....	13
Figure 9. Analytical and Computed Velocity Profiles for Various Hartmann Numbers.	14
Figure 10. Normalized Computed Velocity Profiles for Various Hartmann Numbers ...	15
Figure 11. Surface Temperature over the Analyzed Fluid Domain for $M=0$ .....	16
Figure 12. Calculated Heat Flux for Various Hartmann Numbers .....	16
Figure 13. Heat Flux Normalized to Case 0 .....	17
Figure 14. Pressure over the Analyzed Fluid Domain.....	19

## **ABSTRACT**

Steady state channel flow of an electrically conductive liquid exposed to transverse magnetic and electric fields was analyzed using a finite element model in COMSOL Multiphysics software to determine the flow velocities and heat transfer characteristics of the flow. The Lorentz force, velocity profile, and Nusselt number results were compared to the available exact solutions for this Hartmann flow problem. A range of dimensionless Hartmann numbers in the laminar region was analyzed numerically as well as analytically, and the solutions were compared.

## **1. Introduction**

Magnetohydrodynamics (MHD) is a field that has many applications in metallurgy, microfluidic pumping, power generation in fusion and fission reactors, and cosmic studies. The ability to control the flow of liquid metal and plasmas at high temperatures through magnetic fields without mechanical influence has novel applications. Liquid metal flows can be manipulated with the magnetic field producing effects such as electromagnetic braking that is widely used in the continuous casting of steel, [1]. Additionally, MHD has proven to be an efficient pumping method in microfluidic devices whose scale would typically require significant pressure gradients to achieve adequate flow rates, [2]. A specific type of MHD flow that has been studied extensively is flow in a channel between two parallel plates, known as Hartmann flow. Analytical solutions have been obtained for the flow profile and heat transfer characteristics. Numerical solutions can be obtained through finite element analysis of the magnetic field and flow.

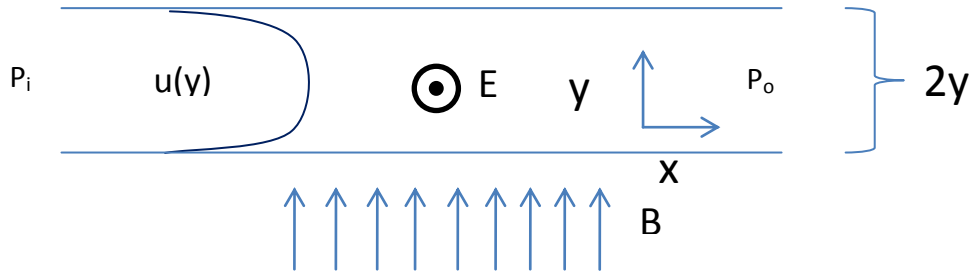
For this project, the flow of a steady state incompressible liquid metal between parallel plates in a transverse magnetic field was analyzed. The plates were assumed to be electrically insulated so as to not influence the magnetic field. A pressure was applied to the inlet of the channel, and a Lorentz body force due to the magnetic field was calculated. The Lorentz force altered the flow profile and consequently the heat transfer characteristics of the flow. The change in heat transfer rate with respect to the change in flow profile due to the Lorentz force was analyzed.

## 2. Methodology

### 2.1 Governing Equations

The Maxwell and Navier-Stokes equations can be solved using the COMSOL Multiphysics analysis software and compared to theoretical solutions found in references [3], [4], and [5]. The problem that was analyzed is shown in Figure 1. The parallel plates were separated by a distance of  $2y_0$ . A magnetic field was applied in the upward  $y$ -direction. A differential pressure between the inlet and outlet of the plates was applied so that a flow profile that varies in the  $y$ -direction develops. The pressure gradient in the  $z$ -direction was chosen as zero so that flow only occurred in the  $x$ -direction. The magnetic field created an electromotive force on the fluid as it moved between the plates.

**Figure 1. Electric and Magnetic Fields Applied to a Pressure Driven Parallel Plate Flow**



The governing equations for this problem are derived from the Maxwell equations, Ohm's law, and the Navier-Stokes equations. The electromotive force needs to be applied as a body force in the Navier-Stokes equations so that the effect of the magnetic field on the fluid is included in the fluid flow solution.

The Maxwell Equations were taken from [5]:

$$\nabla \cdot \mathbf{D} = \rho_e$$

$$\nabla \cdot \mathbf{B} = 0$$

$$\nabla \times \mathbf{E} = -\frac{\partial \mathbf{B}}{\partial t}$$

$$\nabla \times \mathbf{H} = \mathbf{J} + \frac{\partial \mathbf{D}}{\partial t}$$

This was combined with Ohm's Law:

$$\mathbf{J} = \sigma(\mathbf{E} + (\mathbf{V} \times \mathbf{B}))$$



In order to derive an analytical solution from the above equations, certain assumptions must be made. The constitutive equation,  $\mathbf{B} = \mu_0 \mathbf{H}$ , is assumed accurate for liquid metals and gases in most MHD problems, although it is not true in general for all types of flows. This, along with the assumption that induced magnetic fields are much smaller than the externally applied magnetic field and that  $\partial \mathbf{D} / \partial t$  is negligible are the three major assumptions used to reduce the Maxwell equations to an MHD approximation form. These assumptions are generally valid for most ordinary conductors at relative low velocities ( $V \ll$  speed of sound). As shown in detail in Chapter 6 of [5], Maxwell's equations can be reduced using these assumptions to:

$$\nabla \times \mathbf{E} = -\frac{\partial \mathbf{B}}{\partial t}$$

$$\nabla \times \mathbf{H} = \mathbf{J}$$

$$\nabla \cdot \mathbf{J} = 0$$

$$\nabla \cdot \mathbf{B} = 0$$

$$\mathbf{J} = \sigma(\mathbf{E} + (\mathbf{V} \times \mathbf{B}))$$

These equations are coupled with the incompressible Navier-Stokes equations (Chapter 4 of [5]) through the  $\mathbf{J}$  and  $\mathbf{B}$  fields which appear as a body force:

$$\rho \left( \frac{\partial \mathbf{V}}{\partial t} + \mathbf{V} \cdot \nabla \mathbf{V} \right) = -\nabla p + \mu \nabla^2 \mathbf{V} + \mathbf{F}_b$$

Where  $\mathbf{F}_b = \mathbf{J} \times \mathbf{B}$

For the parallel plate problem, the left side of the equation equals zero because velocities in the y and z directions are zero, the velocities are time invariant, and the velocity profile does not change with x. Likewise many terms on the right hand side are zero, and the equations simplify to:

$$0 = -\frac{\partial p}{\partial x} + \mu_f \frac{\partial^2 u}{\partial y^2} - B_0 J_z$$

$$0 = -\frac{\partial p}{\partial y} + J_z B_x - J_x B_z$$

$$0 = -\frac{\partial p}{\partial z} + \mu_f \frac{\partial^2 w}{\partial y^2} - B_0 J_x$$

Using Ohm's Law:

$$J_x = \sigma(E_x - B_0 w)$$

$$J_z = \sigma(E_z - B_0 u)$$

Since we have chosen the flow (and pressure gradient) to be in the x-direction, the  $w$ ,  $J_x$ ,  $E_x$ , and  $\partial p / \partial z$  are zero and the above equations are reduced to the one equation shown below:

$$0 = -\frac{\partial p}{\partial x} + \mu_f \frac{\partial^2 u}{\partial y^2} - B_0 \sigma(E_z - B_0 u)$$

This is a representation of a simple one dimensional parallel plate flow with an applied body force dependent upon the applied electrical and magnetic fields. This equation can be used to solve for the velocity profile between the plates by applying appropriate boundary conditions which are discussed in a later section.

The general energy equation from [6] is solved in order to calculate the temperature distribution and heat flux in the fluid and through the boundaries:

$$\rho \frac{Di}{Dt} - \nabla \cdot k \nabla T - \nabla \cdot \left( \sum_j \gamma_j i_j \nabla m_j \right) - \mu \phi - \frac{DP}{Dt} = S$$

$$\text{where } \phi = \left( \frac{\partial u_i}{\partial x_j} + \frac{\partial u_j}{\partial x_i} - \frac{2}{3} \frac{\partial u_l}{\partial x_l} \delta_{ij} \right) \frac{\partial u_i}{\partial x_j}$$

These equations are rearranged in COMSOL assuming time invariance and no dissipation so that Conduction = Source – Convection:

$$\nabla \cdot k \nabla T = Q - \rho c_p \mathbf{V} \cdot \nabla T$$

After COMSOL solved the above equation, the results were post-processed to solve for the convective heat transfer coefficient.

$$h = \frac{q''}{T_s - T_b} \text{ where } T_b = \frac{\int_{-y_0}^{y_0} (Tu) dy}{\int_{-y_0}^{y_0} (u) dy}$$

The convective heat transfer coefficient was used to determine the Nusselt Number.

## 2.2 Solution Method

### 2.2.1 Lorentz Force Solution

COMSOL Multiphysics was used to create a magnetostatics model of a channel with conductive fluid flow exposed to magnetic and electric fields. The obtained solutions are compared to the analytical solutions for the Lorentz force and fluid velocity shown in the following section. Mercury was selected as the conductive fluid due to its applicability to MHD (a conductive metal that is often used and studied because it is liquid at room temperatures). Fluid properties at 523.15K from [7] were used because the heat transfer was analyzed at temperatures close to this temperature. These properties are presented in Table 1.

Electrical Conductivity	Dynamic Viscosity	Density	Thermal Conductivity	Heat capacity
$1 \times 10^6$ S/m	0.001 Pa*s	13026 kg/m <sup>3</sup>	13.07 W/(m*K)	136 J/(kg*K)

**Table 1. Applicable Fluid Properties of Mercury at 523K**

The flat plates were separated by a distance of 10 centimeters. The length of the modeled plates was 6 meters, which is a sufficient condition to match the assumption used in the analytical solution, that the length is much greater than the distance between the plates. The model was meshed using the built in COMSOL meshing functions. A fine mesh of 23552 triangular elements was used:

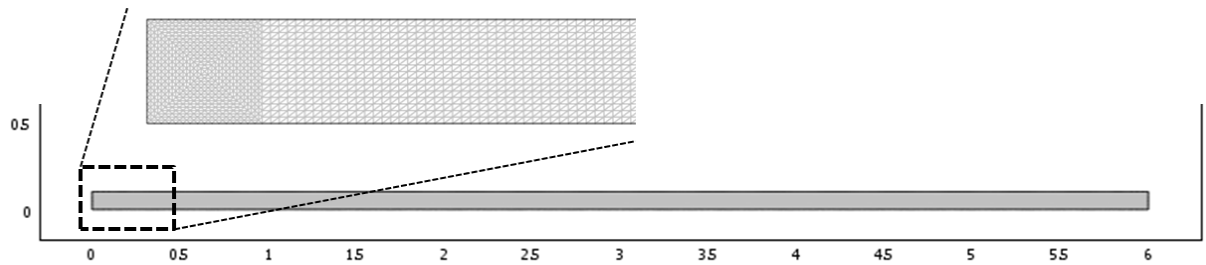


**Figure 2. Meshed Domain**

An electrical insulation boundary condition was applied to the border of the domain as this was assumed in the analytical solution. The boundary conditions are shown in Figure 3.

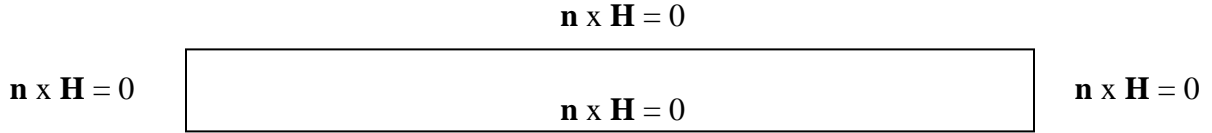


**Figure 3. Applied Magnetostatics Boundary Conditions**

Four magnetic fields of different strength were applied so that multiple flow profiles and Hartmann numbers could be compared to the baseline case (with no magnetic field applied). Table 2 presents the different fields that were evaluated.

**Table 2. Conditions Used to Evaluate the Lorentz Force Contribution**

	Case 0	Case 1	Case 2	Case 3	Case 4
Applied Magnetic Field (T)	0	0.002	0.004	0.006	0.01
Hartmann Number	0	3.2	6.3	9.5	15.8

The analyzed flow is called a Hartmann flow, and the dimensionless number that defines different Hartmann flows is known as the Hartmann Number (M). The definition of the Hartmann number is  $M = y_0 B_0 \sqrt{\sigma / \mu_f}$ .

The magnetic field was applied in COMSOL to the subdomain as an external distributed field in the positive y-direction. This ensures that the magnetic field is in one direction, and is constant within the domain. “Remnant flux density,” is the term in COMSOL that allows the user to directly apply this directional magnetic field,  $\mathbf{B}$ , throughout the domain. Alternatively, the magnetic field could have been applied as boundary conditions, however applying the field in the subdomain allowed for the electrical insulation boundary conditions to be applied instead.

Results of cases with electric fields were evaluated but not included in this project because the Hartmann number is unaffected. The electric field acts similarly to a back-pressure, therefore the profile of the flow remains the same.

The magnetostatics and hydrodynamic solutions were solved for separately, and iteratively. Figure 4 shows the iterative solution method that was used.

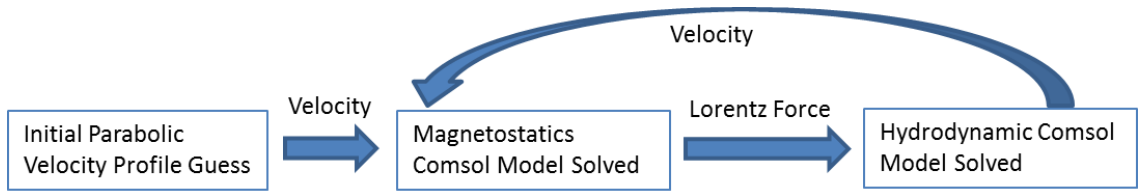


**Figure 4. Iterative Solution Method**

A parabolic flow solution was applied as an initial guess, so that an initial Lorentz force could be solved for and input in the hydrodynamics model. Once the velocity, insulation boundary conditions, and magnetic fields were applied a magnetostatics solution was obtained in COMSOL. COMSOL allows the same model and mesh to be used for both the hydrodynamic and magnetostatics solvers so that variables can be passed easily. The Lorentz force solution was applied to the hydrodynamic model in COMSOL and once the appropriated conditions were applied (discussed further in the next section) a hydrodynamic solution was obtained. The new calculated velocities were then applied to the magnetostatics model and a new Lorentz force was calculated. This process was repeated several times for each case until the change in velocities between iterations was insignificant.

### 2.2.2 Hydrodynamic Flow Solution

The calculated Lorentz force solution is used as an input to the Navier-Stokes equation. The iterative solution method described in the above section was used because simultaneous solution of the hydrodynamic and magnetic equations can cause instability without a close initial guess, especially at the inlet and outlet boundaries. Low pressure inlet conditions with a 0 pressure outlet condition were applied to the 0.1 meter high by 6 meter fluid domain. This ensures low velocities so that end effects and entrance lengths do not dominate the solution. It also ensures that the flow is sufficiently developed within the analyzed region. The boundary conditions are illustrated in Figure 5.

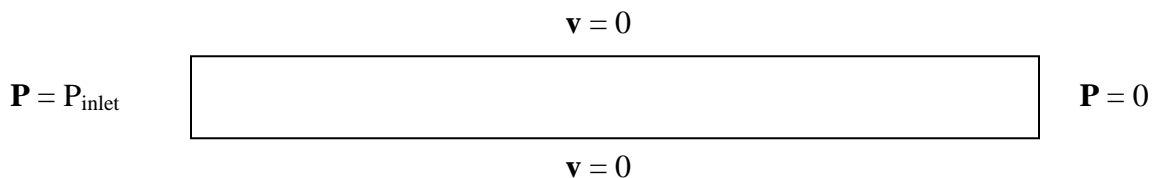


**Figure 5. Applied Fluid Dynamics Boundary Conditions**

No slip wall conditions were applied to the upper and lower plates. The calculated Lorentz force from the magnetostatics solution was applied as a body force to the fluid domain. Different pressures were applied to each case so that the volumetric flow rate between the plates differed by less than 1% between cases. Increased pressures were applied at higher Hartmann numbers to achieve the same flow rate because the Lorentz force acts against the flow. The entrance region affects the linearity of the pressure drop; therefore trial and error was used to get the desired pressure drop per meter in the fully developed region. At higher Hartmann numbers the entrance length is reduced, therefore the analytical equations were used to estimate the required inlet pressure for cases 3 and 4. The following inlet pressures were used:

**Table 3. Conditions Used to Evaluate the Fluid Velocities**

	Case 0	Case 1	Case 2	Case 3	Case 4
Applied Inlet Pressure (Pa)	0.006	0.023	0.071	0.149	0.395
Hartmann Number	0	3.2	6.3	9.5	15.8

The velocities that result from these pressures ensured that the flow is laminar. Figure 6, taken from [8], shows that as the Hartmann number increases, the flow becomes more stable and requires a much higher Reynolds number to transition to turbulent flow. For pressure driven parallel plate flow, transition to turbulent flow is expected to occur at a Reynolds number of 2000, [9]. The Reynolds number for Case 0 is 600 and less for the other cases, therefore laminar flow was present in all cases.

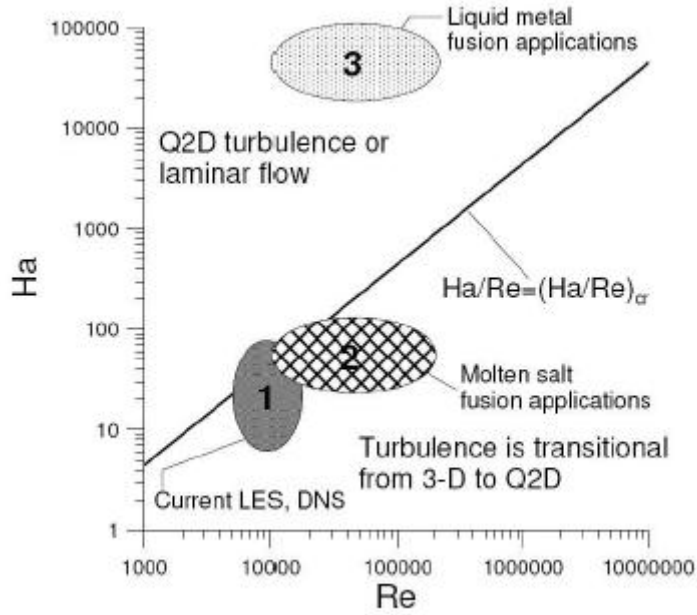


**Figure 6. Transition to Turbulence in Hartmann Flows [9]**

Once the boundary conditions and Lorentz forces were applied to the model, the hydrodynamic problem was solved. As described above, the magnetostatics and hydrodynamic solution were solved iteratively until new solutions stopped changing significantly.

### 2.2.3 Heat Transfer Solution

The forced convection heat transfer solution was obtained by applying the boundary conditions specified in Figure 7 to the geometries in COMSOL.

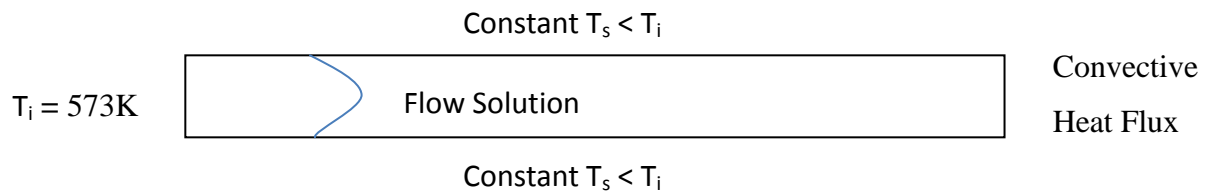


**Figure 7. Applied Boundary Conditions for the Heat Transfer Analysis**

The fully developed analytical fluid flow solutions were used in the heat transfer analysis so that flow entrance effects would not affect the solution. A shorter geometry, 0.1 meter high by 2 meter long fluid domain, was used for the heat transfer solution because the domain quickly reached the wall temperature. The walls were held at a

constant temperature (323.15 K) and the fluid entered at a constant inlet temperature (573.15 K). A convective heat flux boundary condition was applied to the outlet. An additional domain was used for the region from 0 meters to 0.2 meters so that the temperature profile can be integrated in COMSOL at 0.2 meters and a bulk temperature could be determined.

The solutions for each case were compared to determine how the flow profile affects the heat transfer between parallel plates. The Nusselt number was used to determine how the Hartmann number affected the heat transfer rate.

The heating that occurs when the magnetic field is applied to the flow was not included in this analysis because the effect of flow profile on the heat transfer was desired. Reference [3] describes a steady state solution where this heating is set equal to the heat lost through the walls.

### 2.3 Expected Results

The Lorentz force was expected to match the result derived in [5]  $\mathbf{F}_b = \mathbf{J} \times \mathbf{B}$ , which for this specific problem simplifies to  $F_b = -B_0 \sigma (E_z - B_0 u)$ . When no slip boundary conditions are applied at  $y = \pm y_0$ , the velocity profile (assuming a constant pressure gradient, magnetic, and electric field) can be obtained:

$$u = \frac{y_0}{M^2} \left( \frac{1}{\mu_f} \frac{\partial P}{\partial x} + \frac{M}{y_0} \sqrt{\frac{\sigma}{\mu_f}} E_z \right) \left( \frac{\cosh(My/y_0)}{\cosh(M)} - 1 \right)$$

$$M, \text{ Hartmann Number } M = y_0 B_0 \sqrt{\sigma / \mu_f}$$

This is the profile that is expected in the fully developed region of the flow. For increased Hartmann numbers, the flow profile gradually becomes flatter, with steep gradients close to the wall in order to satisfy the no-slip boundary condition.

Increased pressure gradients or increased electric fields that do not affect the applied magnetic field do not change the normalized velocity profile; they only change maximum velocity at the center of the channel. Increased pressure gradients are required to keep the maximum velocities similar when analyzing different Hartmann numbers because the Lorentz force caused by the magnetic field will work against the motion of the fluid in this analysis,.



It can be expected that the heat transfer for the higher Hartmann number flows of the same volumetric flow rate will be increased due to the increase flow near the wall boundary. Increased convection would be expected because the increase in velocity is near the boundary. The point of greatest heat flux at the inlet is at the walls (since the wall temperature is held constant.) The dimensionless Nusselt number is a common parameter used to characterize the convective heat transfer for a specific type of flow. As described in [10], for the baseline condition with no magnetic field (Case 0) the expected Nusselt number is 7.54. Laminar fully developed flow in a rectangular cross section pipe of infinite width is assumed for this theoretical result. Case 0 is used to confirm accuracy of solution and conformance to theory. The other cases were compared to this result to examine the change in heat transfer rate. Nusselt numbers will be calculated for each case.

### 3. Results and Discussion

#### 3.1 Lorentz Force Solution

The magnetostatics finite element modeling module of COMSOL Multiphysics was used to determine the Lorentz force for a Hartmann flow described by the boundary conditions shown in Figure 3. A 2-dimensional 0.1 meter high, 6 meter long domain was analyzed with the applied magnetic fields and hydrodynamic solutions described in section 2.2 and repeated in the Table 4.

**Table 4. Conditions Used to Evaluate the Magnetic and Hydrodynamic Models**

	Case 0	Case 1	Case 2	Case 3	Case 4
Applied Inlet Pressure (Pa)	0.006	0.023	0.071	0.149	0.395
Applied Magnetic Field (T)	0	0.002	0.004	0.006	0.01
Hartmann Number	0	3.2	6.3	9.5	15.8

The hydrodynamic and magnetic solutions were solved iteratively since the velocity affects the magnetic solution, and the Lorentz force affects the velocities. As shown in Figure 8, with an increasing Hartmann number, the Lorentz force increases and matches the expected results. The lines represent the exact solution described in section 2.3. The dots are the results of the COMSOL model.

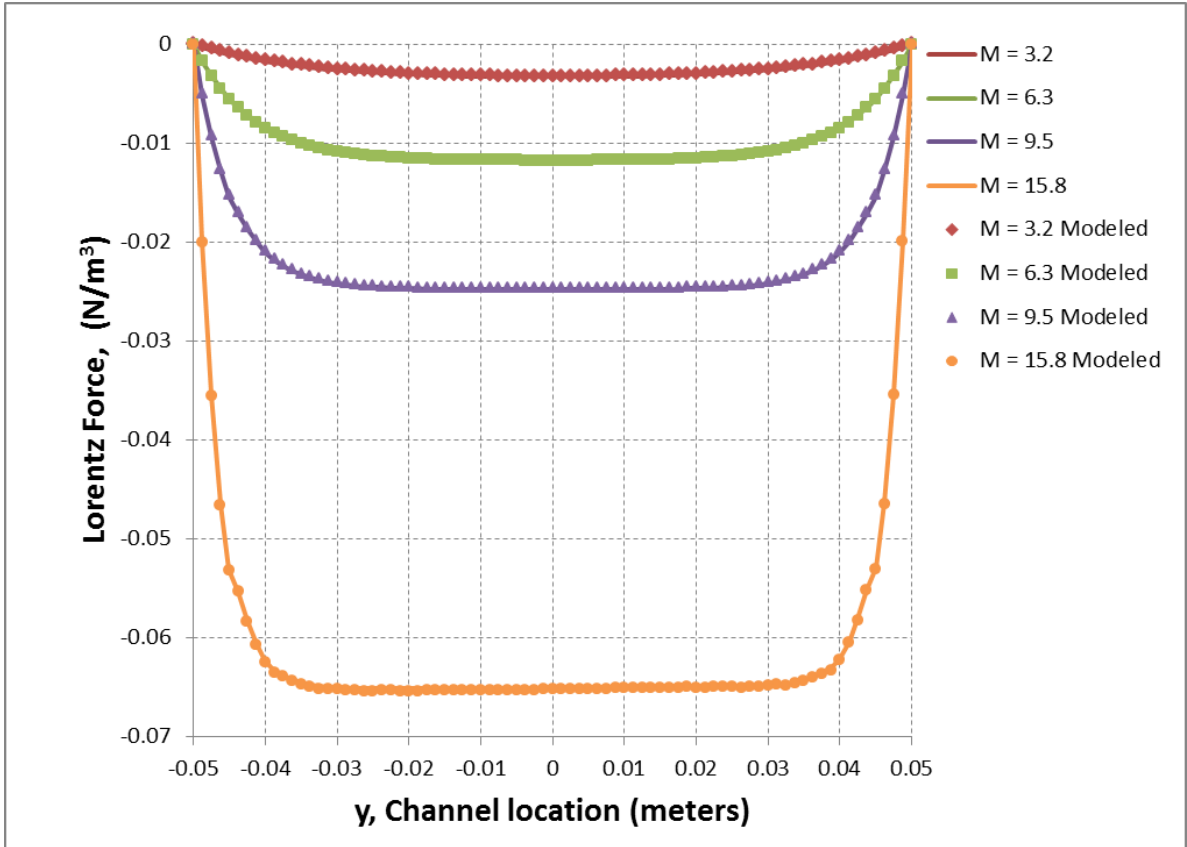


**Figure 8. Calculated and Exact Lorentz Force Solutions**

The body force is divided by the length of the channel to determine the equivalent back pressure that is being applied to the fluid. Toward the middle of the channel, the force almost negates the applied pressure force, which results in very low velocities in the channel when compared to a solution with no applied magnetic field. Figure 8 confirms that the analytical Lorentz body force  $-B_0\sigma(E_z - B_0u)$  matches the calculated results. Therefore this term can be directly used in the fluid flow solution so that the magnetic solution does not need to be recalculated or solved iteratively. However, for more complicated flows with non-uniform fields such a simple term may not be readily available or determined, therefore the iterative method used in this project is a more powerful solution method for more general, realistic flows.

### 3.2 Fluid Flow Solution

The calculated velocity profiles for a pressure driven flow for the cases described in Table 4 are shown in Figure 9. These profiles have approximately the same volumetric flow rate (within 1%).

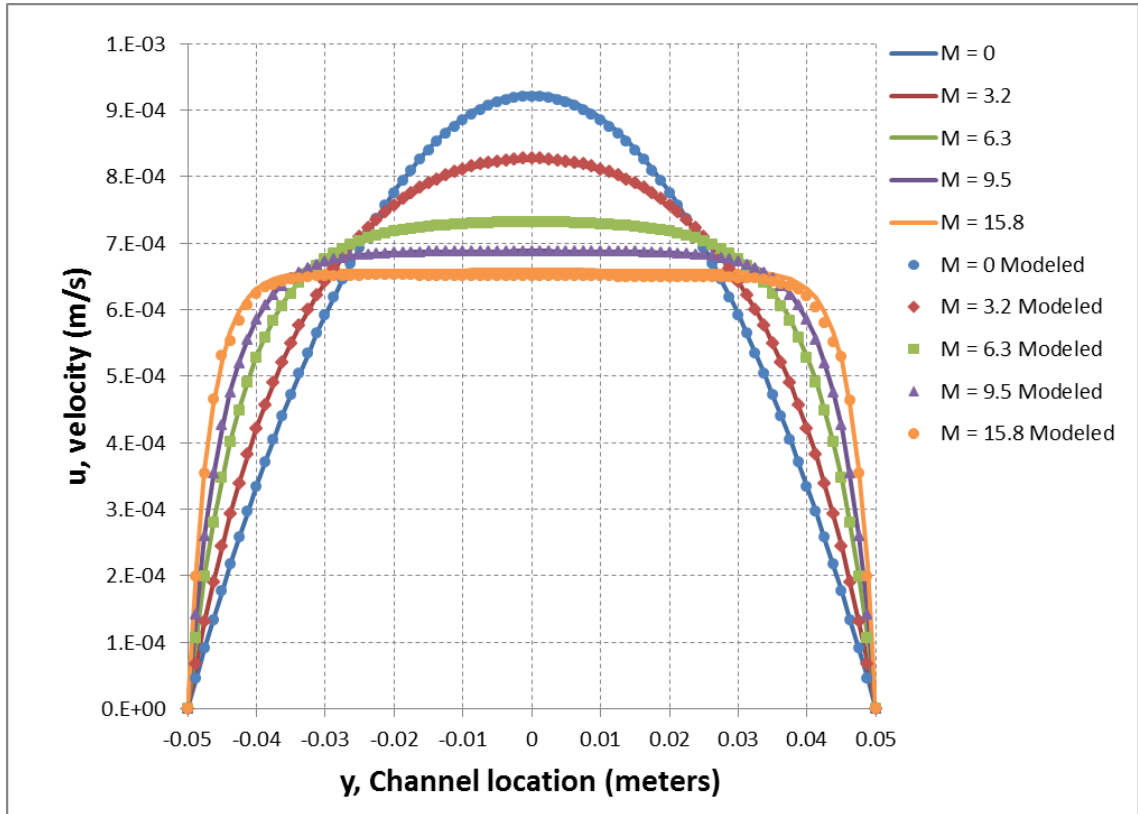


**Figure 9. Analytical and Computed Velocity Profiles for Various Hartmann Numbers**

As the magnetic field was increased, the Lorentz force also increased, which reduces the velocity throughout the channel. The Lorentz force is a function of velocity, therefore the normally parabolic flow receives a greater counter-flow force at the highest velocity points (center of the channel). As the magnitude of the magnetic field increases, the force in the center increases until the flow becomes almost constant through the channel (except very close to the walls so the solution satisfies the no slip boundary condition). Contour plots of the pressure field combined with an arrow plot of the velocity field for each of the analyzed cases are shown in Appendix A. The velocities normalized to the maximum velocity are shown in Figure 10.

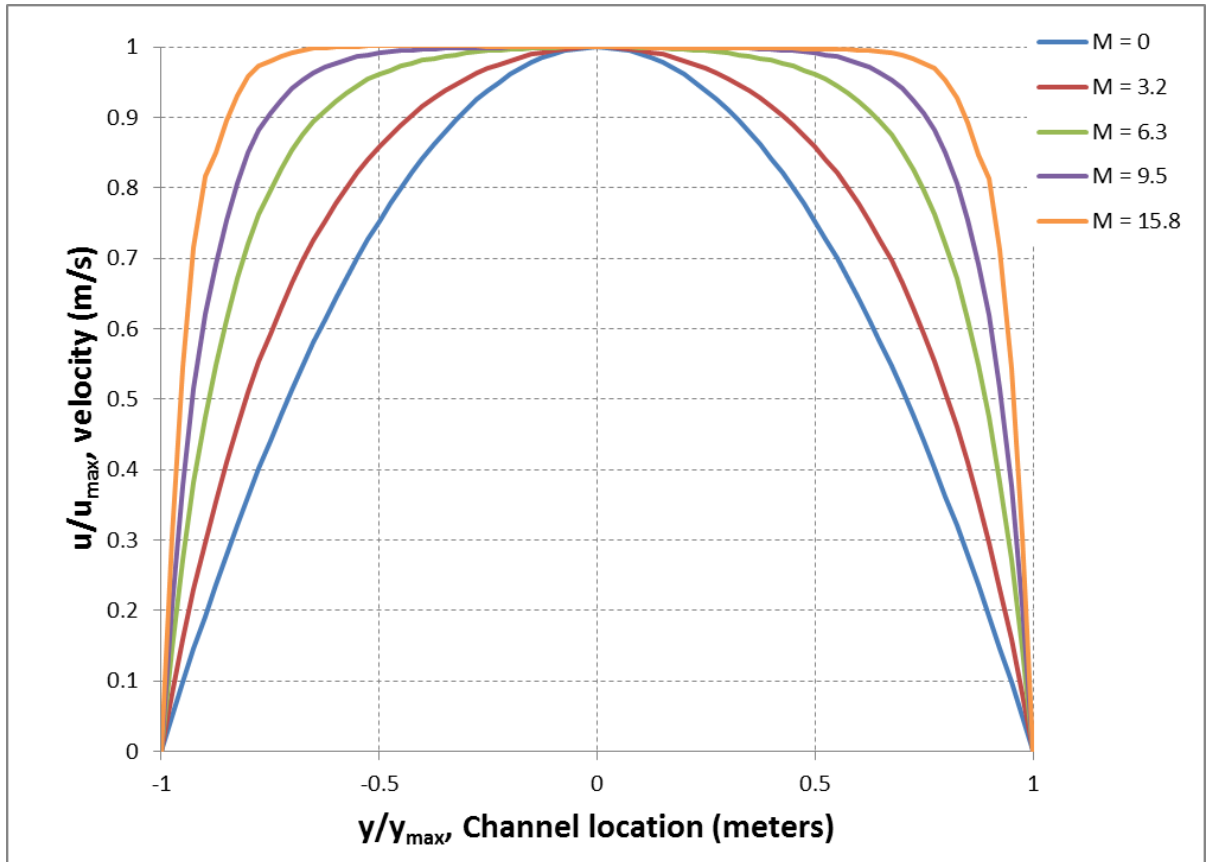


**Figure 10. Normalized Computed Velocity Profiles for Various Hartmann Numbers**

As shown in Figure 10, the effects of the magnetic field become more pronounced as the field increases. Even at the moderate Hartmann numbers used in this project, the velocity profile is nearly flat. Hartmann numbers for many industrial and laboratory applications can be large ( $M = 10 - 10000$ ), [11]. For these flows the velocity profile is practically constant between the plates.

### **3.3 Heat Transfer Solution**

The heat transfer analysis described in Section 2.2.3 was performed. As expected, the heat transfer was enhanced at higher Hartmann numbers with volumetric flow rate held constant. A contour plot of the fluid temperatures for the baseline Case 0 with no applied magnetic field is shown in Figure 11.

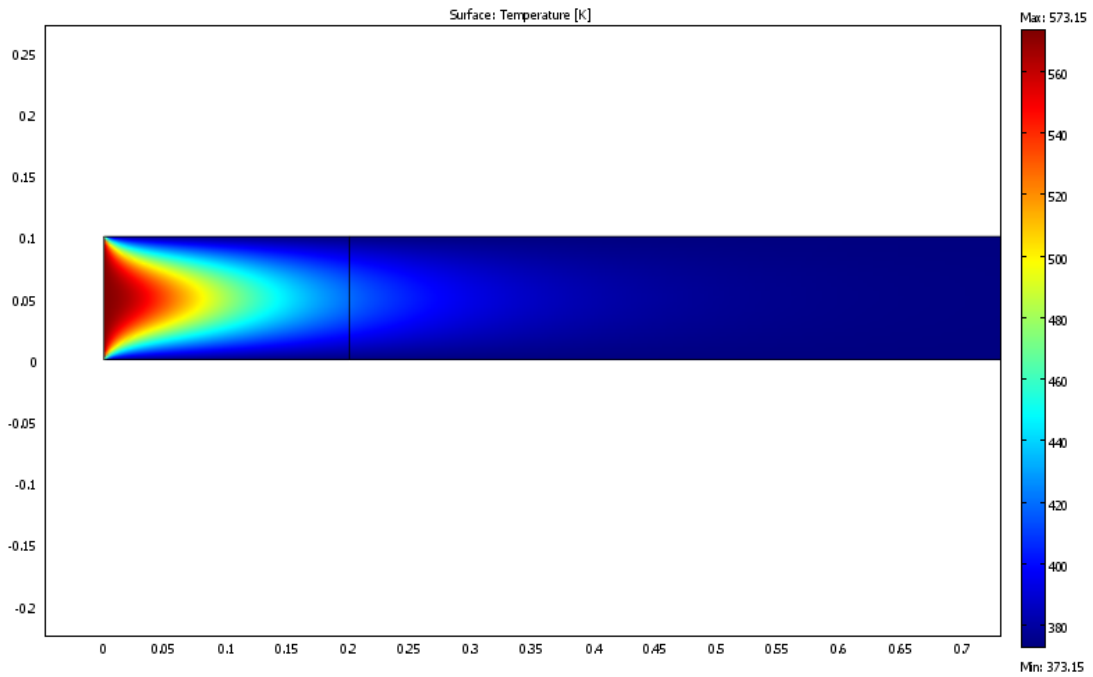


**Figure 11. Surface Temperature over the Analyzed Fluid Domain for M=0**

The temperature contour plots for cases 1-4 were similar to the baseline case. The heat fluxes through the wall for each case are plotted together in Figure 12.

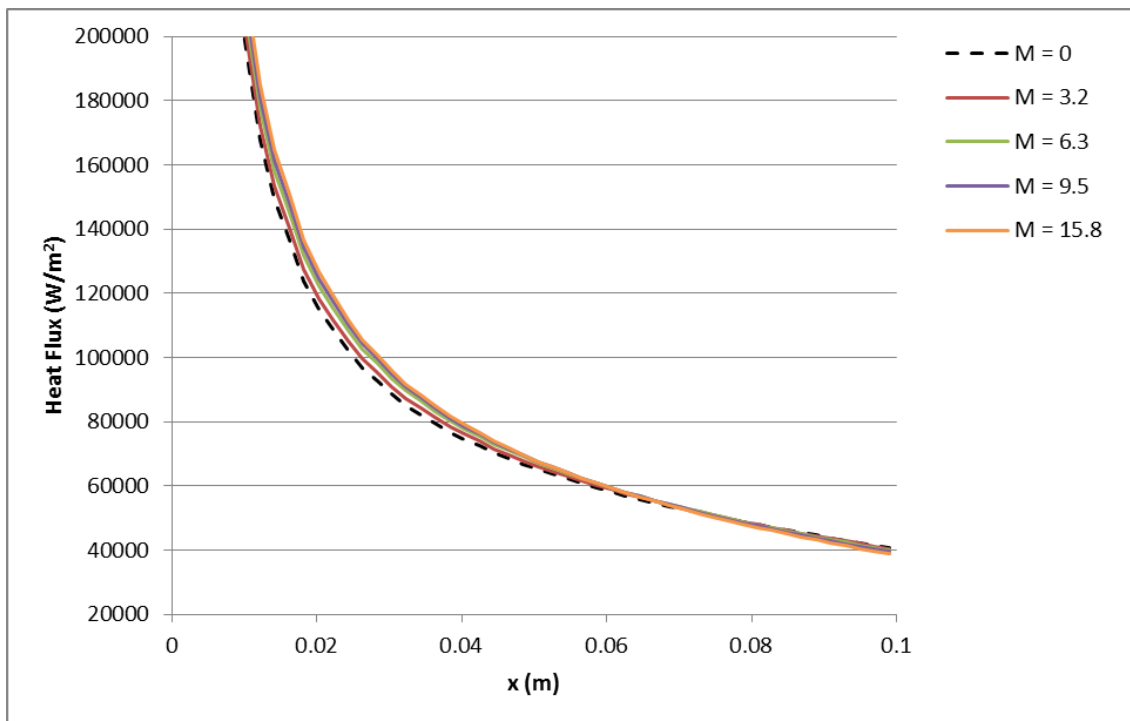


**Figure 12. Calculated Heat Flux for Various Hartmann Numbers**

As shown in the Figure, the heat flux is slightly enhanced with increasing Hartmann Number. Since the heat transfer is enhanced, the temperatures in the fluid domain more quickly reach the wall temperature. A crossover point at approximately 0.08 meters is due to the lower difference in bulk temperature and wall temperature. This is shown more clearly in a normalized plot, Figure 13.

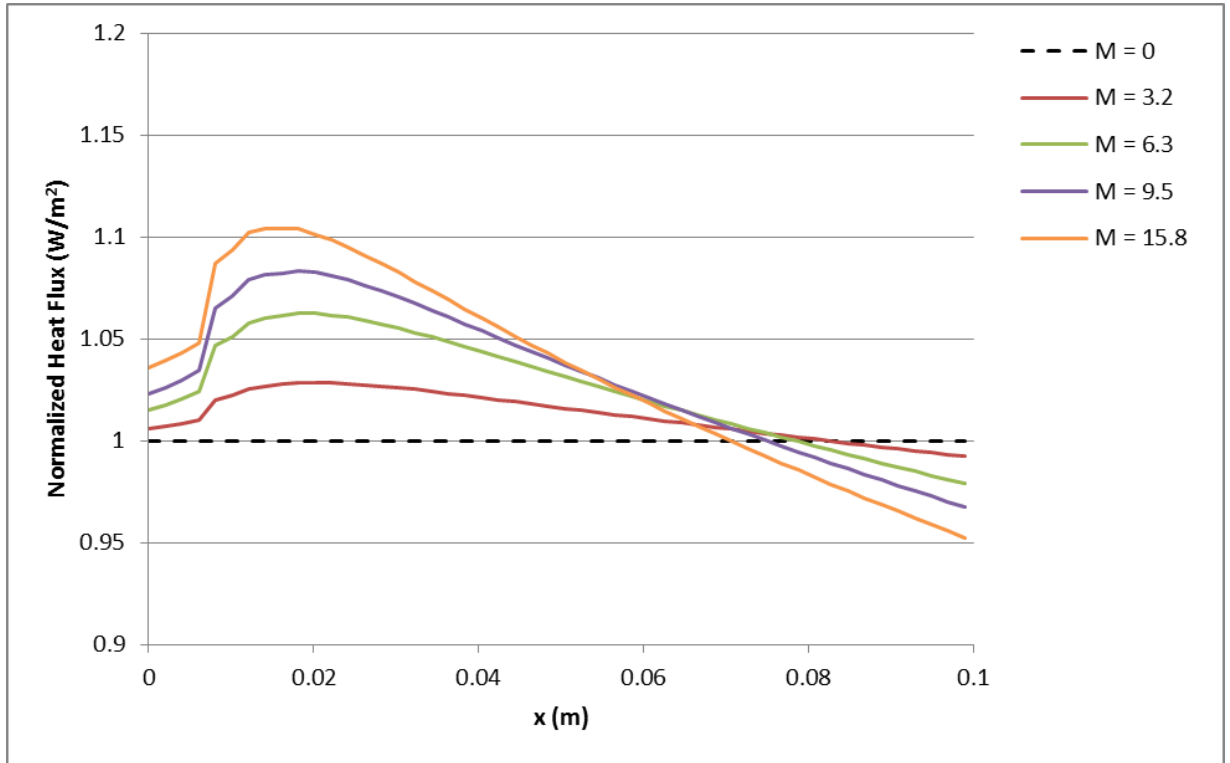


**Figure 13. Heat Flux Normalized to Case 0**

Figure 13 shows the heat fluxes normalized to the baseline Case 0. Ignoring the end effect, the heat flux amplification is a maximum at the beginning of the domain, where temperatures between cases are almost identical due to the inlet temperature boundary condition. Due to the larger heat flux, Cases 1-4 cool faster than Case 0. At  $\approx 0.08$  meters the Hartmann flow cases have cooled to a point where the decreased temperature difference has counteracted the increased heat transfer coefficient, and the overall heat flux is equivalent to the baseline case. The overall heat transfer throughout the domain, however, has been greater.

The heat flux and temperatures were exported from the COMSOL program and post-processed in Microsoft Excel to determine the heat transfer coefficient and Nusselt number. Applicable heat transfer parameters for the solution at  $x = 0.2$  meters (which is

at the edge of the thermal entry length region) are shown in Table 5. This short distance was chosen because the fluid domain quickly reaches the wall temperature due to the relatively high heat transfer coefficient.

**Table 5. Post-processed Heat Transfer Results**

		Case 0	Case 1	Case 2	Case 3	Case 4
Surface Temperature	$T_{inf}$ (K)	373.15	373.15	373.15	373.15	373.15
Heat Flux	$q''$ (W/m <sup>2</sup> )	17415	16526	15444	14787	14117
Bulk Temperature	$T_{bulk}$ (K)	408.31	404.99	401.47	399.60	397.89
Heat Transfer Coefficient	$h$ (W/m <sup>2</sup> *K)	495.3	519.0	545.3	559.1	570.6
Nusselt Number	Nu	7.579	7.941	8.344	8.555	8.731

The Nusselt number exact solution for a parabolic pressure driven channel flow with a constant wall temperature is  $Nu = 7.54$ , [10]. Table 8-9 from [6] shows that a slightly increased Nusselt number is expected in this region of flow. The dimensionless entry length ( $x^+$ ) is 0.033 for Case 0. As shown in Table 6, the calculated Nusselt number is reasonable for the baseline case.

**Table 6. Nusselt Numbers for Parallel Plate Flow Versus Entry Length**

$X^+ = 2*(x/D_h)/RePr$	Nu
0.01	8.52
0.02	7.75
0.05	7.55
0.1	7.55
0.2	7.55

The computed Nusselt number for Case 0 is very close to the exact Nusselt number which gives confidence that the model is accurately predicting the temperature distribution and heat flux in the fluid.



## 4. Conclusions

### 4.1 Applicability of COMSOL to MHD Flows

The results obtained using COMSOL to model a pressure driven parallel plate flow exposed to an external magnetic field were compared to theory and analytical solutions. Convergence issues were encountered when trying to solve both the magnetic and hydrodynamic solutions simultaneously, however when solved iteratively the solutions converged easily. It was discovered that, entrance and end effects can have large influences on both the convergence and the accuracy of the solution. A graph of the pressure on the centerline of the channel for the baseline case with no magnetic field shows that the pressure loss in the entrance region is not linear.

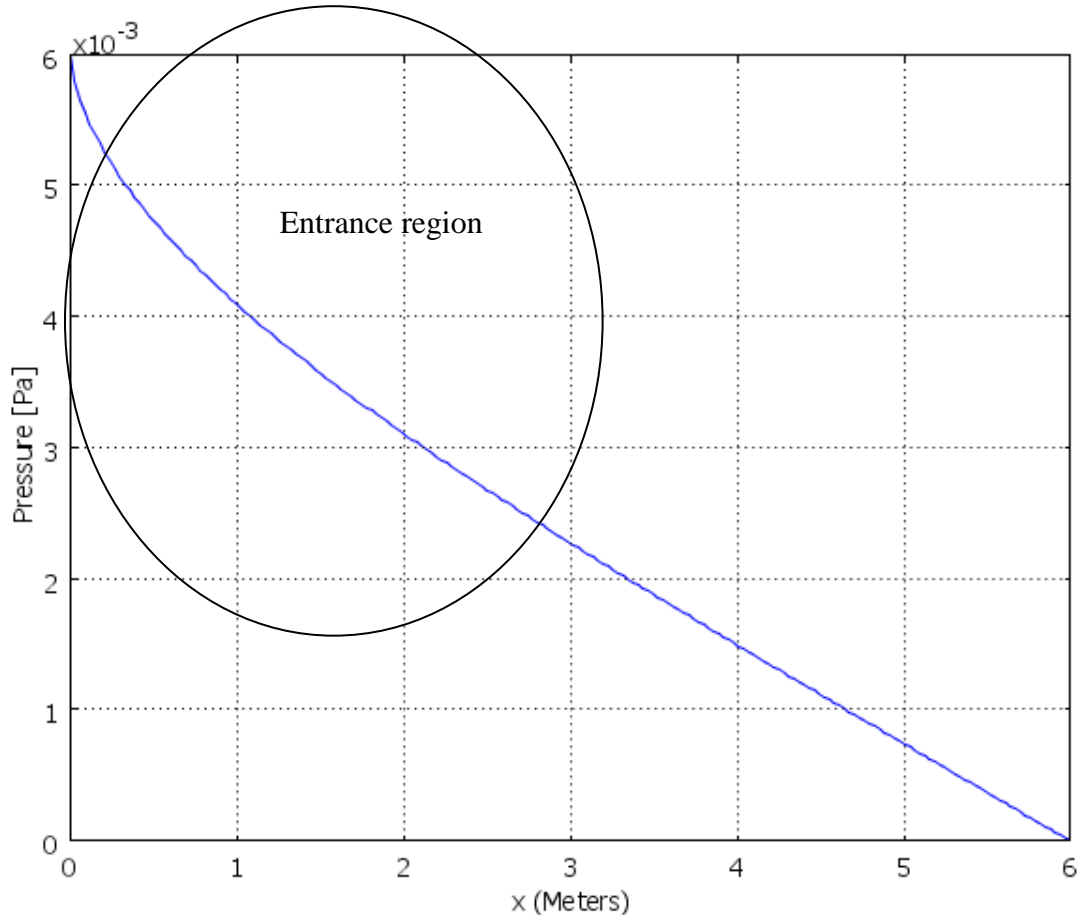


Figure 14. Pressure over the Analyzed Fluid Domain

The purpose of this project was to analyze fully developed flow; therefore the inlet pressure was adjusted until the desired pressure drop in the fully developed region was

achieved. According to [6], the entrance length for parallel plate flow is calculated to be  $0.05 \cdot \text{Re} \cdot D$ , which for the baseline flow, Case 0, would be approximately 3 meters. The measured pressure gradient in the 4 to 6 meter region was therefore used in the exact solutions. The velocities and resulting Reynolds number in this analysis were chosen to be small so that the entrance length of the flow could be kept small. This resulted in some of the analyzed region being fully developed. In the fully developed region, the COMSOL results matched the analytical solutions for the Lorentz force and velocity profile. Given the accuracy of the results obtained from this analysis, it is expected that other Hartmann flows modeled in COMSOL for different conductive fluids would yield accurate results given an appropriate domain size and mesh resolution. Also, it is expected that more complicated MHD flows could be analyzed in COMSOL by using the iterative method that was used to evaluate the flows in this report.

## **4.2 Heat Transfer in Hartmann Flows**

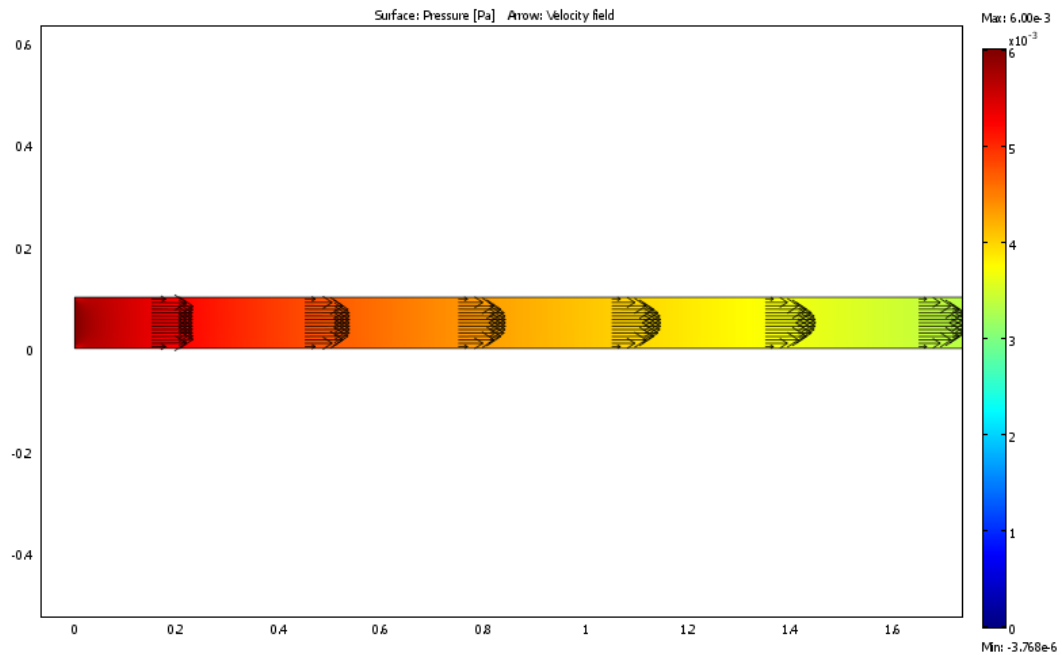
As expected, slightly enhanced heat transfer was obtained at higher Hartmann numbers. This enhancement may be beneficial in flows where magnetic fields are used for braking because Joule heating can cause the temperature of the fluid to rise rapidly. Typically the conductive heat transfer coefficient for liquid metal flows is large, therefore the slight enhancement in heat transfer may be insignificant for practical applications. However for temperature critical applications, the change in Nusselt number for different Hartmann numbers needs to be taken into consideration.

## 5. References

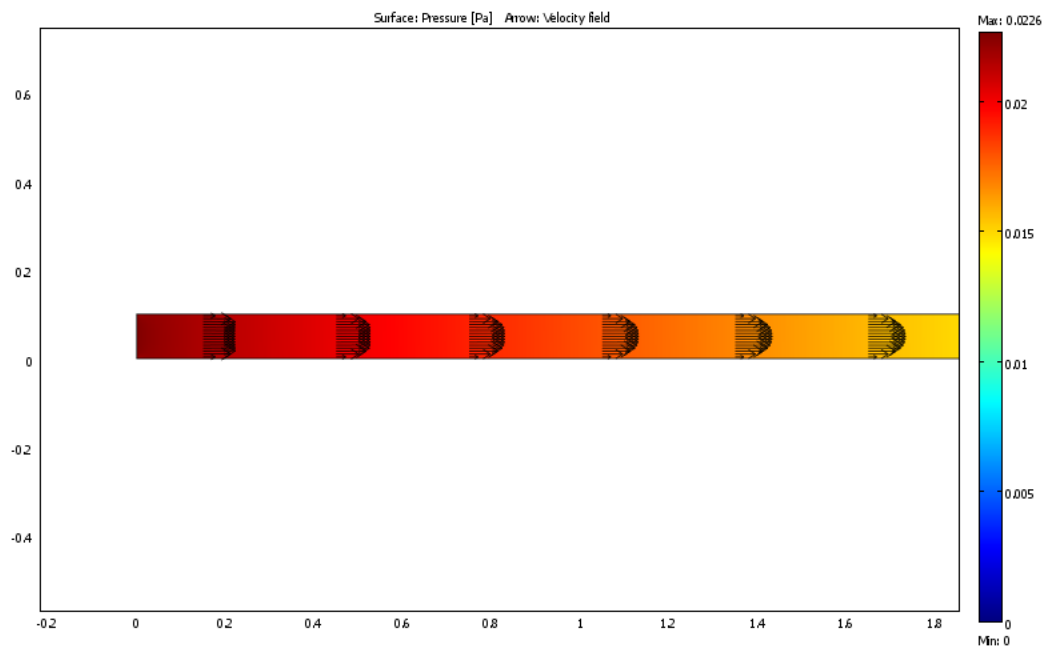
- [1] Egbert Zienicke, Thomas Boeck, and Dmitry Krasnov, Transition to Turbulence in Magnetohydrodynamic Channel Flow of Liquid Metals, NIC Series, Vol. **32** (2006), p. 341-348.
- [2] Asuncion V. Lemoff and Abraham P. Lee, An AC Magnetohydrodynamic Micropump, Sensors and Actuators B: Chemical Vol. 63, Issue 3 (2000), p. 178-185.
- [3] Elmārs Blūms, Yu. A. Mikhailov and R. Ozols, Heat and Mass Transfer in MHD Flows, World Scientific Publishing, 1987.
- [4] R. A. Alpher, Heat Transfer in Magnetohydrodynamic Flow Between Parallel Plates, International Journal of Heat and Mass Transfer Vol. **3** Issue 2 (1961), p. 108-112.
- [5] W. F. Hughes and F. J. Young, The Electromagnetodynamics of Fluids, John Wiley & Sons, New York:1966.
- [6] William Kays et. all, Convective Heat and Mass Transfer Fourth Edition, McGraw-Hill, Boston: 2005.
- [7] Mercury- Properties, The Engineering ToolBox,  
[http://www.engineeringtoolbox.com/mercury-d\\_1002.html](http://www.engineeringtoolbox.com/mercury-d_1002.html)
- [8] S. Smolentsev and R. Moreau, Modeling quasi-two-dimensional turbulence in MHD duct flows, Center for Turbulence Research Proceedings of the Summer Program 2006 p. 419-430.
- [9] Frank M. White, Viscous Fluid Flow Third Edition, MaGraw-Hill, New York: 2006.
- [10] Frank P. Incropera et. all, Fundamentals of Heat and Mass Transfer 6<sup>th</sup> Edition, John Wiley & Sons, 2007.
- [11] J. C. R. Hunt and R. Moreau, Liquid-metal magnetohydrodynamics with strong magnetic fields: a report on Euromech 70, Journal of Fluid Mechanics, Vol. 78 (1976), p. 261-288.

## **6. Appendix A: Additional Graphs of Solutions**

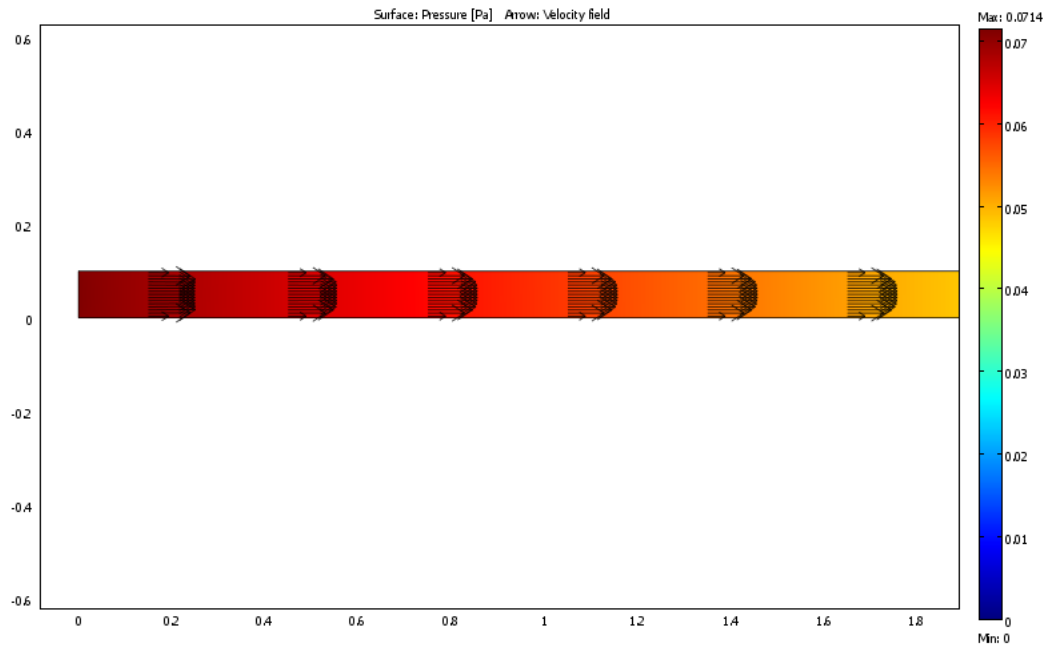
Contour plots showing the pressure and arrow plots showing the velocity profile for cases 0-4 are shown below. The change in velocity to a flatter profile can be seen. Additionally, the entry length as the Hartmann number increases gets shorter.



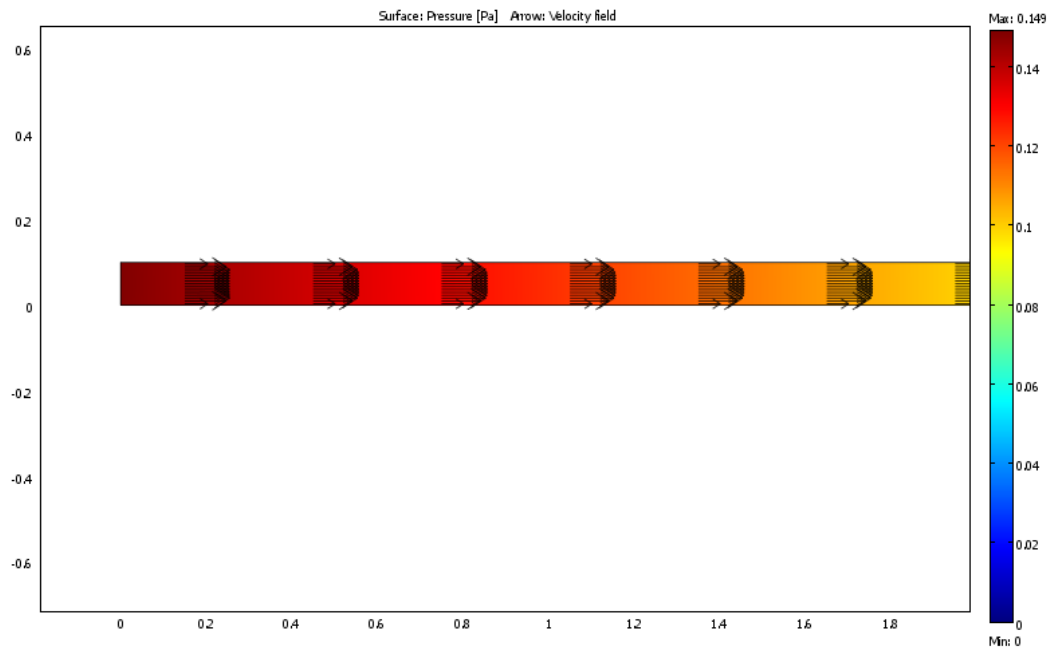
Case 0 Pressure and Velocity Profile Results (M=0)



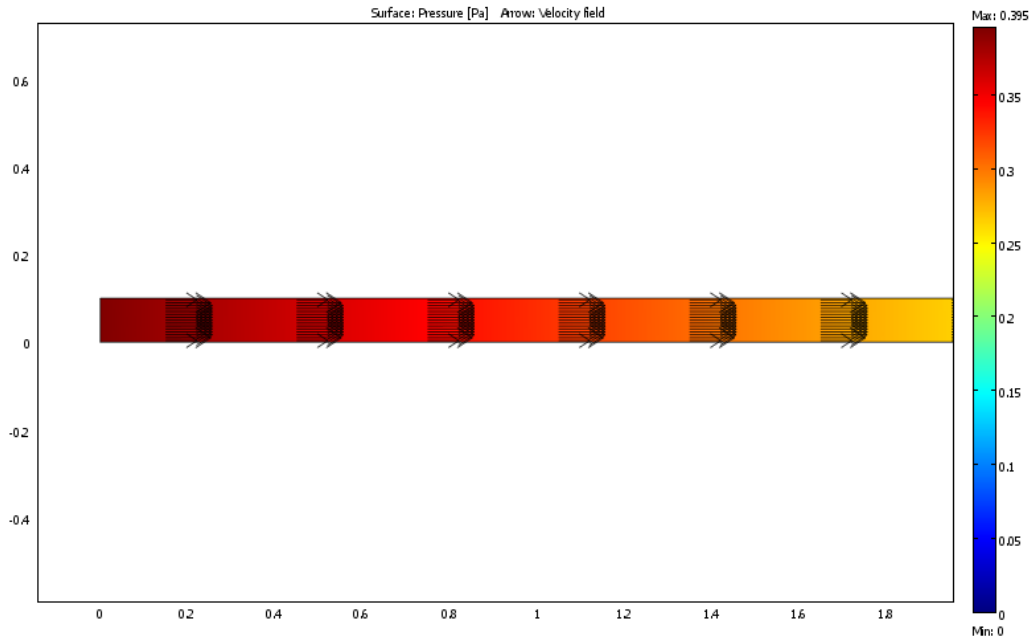
Case 1 Pressure and Velocity Profile Results (M=3.2)



Case 2 Pressure and Velocity Profile Results ( $M=6.3$ )



Case 3 Pressure and Velocity Profile Results ( $M=9.5$ )



Case 4 Pressure and Velocity Profile Results (M=15.8)